

Noise Suppression in Ultrasound Beamforming Using Convolutional Neural Networks

By

Zhanwen Chen

A thesis submitted in partial satisfaction of the
requirements for the degree of
Master of Science

in

Computer Science

in the

Graduate Division

of the

Vanderbilt University

Committee in charge:

Assistant Professor Matthew Berger, Chair
Assistant Professor Maithilee Kunda

Fall 2019

The thesis of Zhanwen Chen, titled Noise Suppression in Ultrasound Beamforming Using Convolutional Neural Networks, is approved:

Chair	_____	Date	_____
	_____	Date	_____
	_____	Date	_____

Vanderbilt University

Noise Suppression in Ultrasound Beamforming Using Convolutional Neural Networks

Copyright 2019

by

Zhanwen Chen

Abstract

Noise Suppression in Ultrasound Beamforming Using Convolutional Neural Networks

by

Zhanwen Chen

Master of Science in Computer Science

Vanderbilt University

Assistant Professor Matthew Berger, Chair

To my parents, Cheng Yuehong and Chen Feng. Thank you for years of unconditional support and encouragement.

Contents

Contents	ii
List of Figures	iv
List of Tables	v
1 Introduction	1
1.1 Introduction to Ultrasound Beamforming	1
1.2 Challenges in Ultrasound Beamforming	4
1.2.1 Off-Axis Scattering	5
1.2.2 Reverberation	6
1.3 Noise Suppression Algorithms	6
1.4 Contribution	7
1.5 Organization	7
2 Background	8
2.1 Classic Acoustic Clutter Suppression Algorithms	8
2.1.1 Tissue Harmonic Imaging	8
2.1.2 Time-Reversal Technique	9
2.1.3 Second-Order Ultrasound Field	9
2.1.4 Short-Lag Spatial Coherence	10
2.1.5 Coherence Factor	11
2.1.6 Minimum-Variance Beamforming	11
2.2 Machine Learning-Based Acoustic Clutter Suppression Algorithms	12
2.2.1 ADMIRE	12
2.2.2 Beamforming Through Regularized Inverse Problems in Ultrasound Medical Imaging	12
2.3 Deep Learning-Based Acoustic Clutter Suppression Algorithm	13
2.3.1 Introduction to Neural Networks	13
2.3.2 Multi-Layer Perceptrons for Suppressing Off-Axis Scattering	14
2.3.3 Convolutional Neural Networks for Noise Reduction	14

Bibliography**15**

List of Figures

List of Tables

Acknowledgments

I want to thank my PI Brett Byram. I want to thank my thesis advisor, Dr. Matthew Berger.

I want to thank my colleague Chris Khan for tirelessly explaining the basics of ultrasound.

Chapter 1

Introduction

1.1 Introduction to Ultrasound Beamforming

Diagnostic medical ultrasound has its roots in sonar and ultrasonic metal flaw detectors. It is a noninvasive, affordable, portable, and real-time method to characterize the cross-sectional view of soft tissues compared with other imaging modalities such as computed tomography (CT) and magnetic resonance imaging (MRI). The underlying principle of ultrasound is the measurement of time elapsed between sending a signal and receiving its echo; given the sound speed *a priori*, we can thus calculate the distance to an object based on this duration.

Ultrasound imaging consists of three steps: emitting sound waves (transmit), receiving echoes (receive), and interpreting those responses to form an image. The transmit step is achieved with ultrasonic transducers - devices that convert electricity into ultrasound waves or vice versa. These same transducers are utilized to receive ultrasonic echoes.

In practice, ultrasound scans are acquired with an array of transducers and each transducer element's pulse transmission is precisely timed by a computer.


The most basic case of ultrasound imaging is plane wave imaging, where all transducers in an array emit the same acoustic pulses at the same time, forming a flat wavefront. After the transmit event, the waves propagate through the field of view and are scattered back to the transducers as pulse-echo responses.

In the case of plane wave imaging, each transducer element samples its measured acoustic pressure at each timestep within a small time window. The distance to an object is then calculated as

$$depth = \frac{sound\ speed * time}{2}$$

Accounting for both directions of travel. With this relationship, the time dimension can be translated to the distance or the depth dimension during the processing step. Thus, each transducer has a series of electric signals v for each depth, y . With a horizontal or lateral series of x transducers, we have a 2D matrix with each value $v = V[x, y]$ representing the electric energy (in volts or V) measured by the x th transducer element at time t . The log-compressed and normalized envelope¹ of this matrix, with its unit in decibels (dB), becomes an image of width x and height y , where each pixel represents the relative intensity in the dynamic range of measured acoustic energy. A typical dynamic range is 60dB. This image modality is called brightness mode, or B-mode.


¹footnotes explaining log compressed envelope w.r.t. dB

Ultrasound relies on scattered waves (echoes) which only occur at aces between varying acoustic impedance. Conversely, if the field of view contains a single, even medium such as air, no signal is returned to the transducers.

Now consider the nontrivial example of plane wave imaging of a phantom, which is an artificial composite of materials of various shapes and acoustic impedance. As is the case previously, all elements emit the same pulse at the same timesteps. However, as each pulse wave travels through the composite, it encounters varying impedance, and some of the wave energy gets scattered at various points in depth and at various degrees, depending on the location and the impedance of the component materials. The returning signals that result from this scattering are used to form a tomographic view of the phantom.

Compared with plane wave imaging, focused transmit provides better signal-to-noise ratios. The rationale for focused imaging is that responses from adjacent transducer elements are more relevant than those farther away. In practice, focus in ultrasound requires a subgroup of the total transducer array to form a single 1D depth-signal series, as opposed to one series for each element. A set of time-delayed (focused) transducer waves are called a beam. Focused imaging maximizes signal, minimizes noise, and results in a higher signal-to-noise ratio. Beamforming can also be viewed as a method for spatial filtering, it gives us spatial selection over where the energy returns from.

To achieve focusing, we first select a subset of transducers (called an *aperture*) and slide the selection by one element for *num_beams* times, where *num_beams* is the configurable number of beams in the overall array. This results in a new channel/aperture dimension to

our data, in addition to the depth and lateral ones. We call this new type of data matrix *channel data* 

Within each subset, we need to send out a focused wave of a curved wavefront by taking advantage of wave interference. The superimposition of waves can cause constructive or destructive interferences, depending on their relative phases and amplitudes upon contact. We preset a focus (typically controlled by a knob on an ultrasound machine), from which we then use a Pythagorean-like calculation to compute the delays we need.

The processing of channel data in order to form an image is called beamforming. The most basic method of beamforming is delay and sum (DAS). We time-delay the data after receiving in order to adjust for the path length differences between the returning wavefront and the transducer elements. After applying delays, we finally operate on the channel dimension. The dimension of our post-delayed channel data is $[depth, elements_per_channel, num_beams]$. To form each beam (vertical slice in the final image), we collapse its channel dimension by summing all 1D transducers responses in its aperture group, resulting in a new data matrix of size $[depth, num_beams]$, called beamformed radio frequency (RF) data. The log compressed envelope (amplitude profile) of the normalized beamformed RF data is the resulting image.

1.2 Challenges in Ultrasound Beamforming

Although widely accepted, DAS beamforming is not an ideal method for clinical application due to the presence of many noises or artifacts, of which we present two: off-axis scattering

and reverberation.

Underlying these two artifacts is the basic mechanism of ultrasound - scattering. Scattering describes the reflection of an acoustic wave as it encounters the boundary between matters of differing impedance. There are many scatters (boundaries) in the field of view. We assume that a wave scatters once before returning to the transducer array and that a transducer subarray emits a straight wave aimed linearly down. However, these assumptions are not always true. The unintended behaviors of scattering lead to artifacts such as off-axis scattering and reverberation clutter.

1.2.1 Off-Axis Scattering

The first such artifact is off-axis scattering. We typically assume that pulse-waves propagate downward, but in reality, pulse waves exhibit diffraction when emitted by a transducer beam. The diffraction resembles the way sound travels. Using an analogy, when person A shouts a secret message facing person B, a bystander C can often hear the message as well (if less clearly). In ultrasound, this phenomenon can be illustrated by beam plots - the normalized far-field magnitude of the transmit pressure versus observation angle. The acoustic pressure we want to focus on is the mainlobe, and the sidelobes are the diffractions that dilute the energy and cause off-axis echoes that degrade the image.

1.2.2 Reverberation

Another cause of image degradation is reverberation or multipath scattering. We assume that when a wave encounters a boundary, it is reflected back to and only to the transducers. However, in reality, the scattered wave can travel in all directions. In addition, the divergent scattered waves can be further scattered by boundaries outside the ROI of the emitting beam. As a result of bouncing around in the field of view, the returning signal gets registered to deeper depths because it takes longer to return to the transducer.

1.3 Noise Suppression Algorithms


Many algorithms have been developed to address ultrasound artifacts. Earlier methods include Tissue Harmonic Imaging, Time-Reversal Technique, Second-Order Ultrasound Field, Minimum-Variance Beamforming, coherence factor, generalized coherence factor, and Short-Lag Spatial Coherence[1]. Aperture Domain Model Image REconstruction (ADMIRE) developed by Byram and Dei [2]. Machine learning approaches tend to work well, but they are too computationally demanding to be real-time, although progress has been made to improve its performance.

In addition, studies have shown that deep neural networks are effective in suppressing noise sources. Of particular relevance is the application of multilayer perceptrons (MLPs) in the aperture domain or channel dimension [3]. Lastly, convolutional neural networks (CNNs) have also been used in biomedical imaging in general [4] and various ultrasound

imaging modalities [5]. In terms of ultrasound beamforming, work has been done using CNNs to learn the entire beamforming process [6].

1.4 Contribution

No one has applied Convolutional Neural Networks on the STFT-domain data.

The aim of this thesis is to investigate the effectiveness of convolutional neural networks (CNNs) in suppressing off-axis scattering and reverberation clutter. Particularly, I apply CNNs to signals in the aperture short-time Fourier transform (STFT) domain to avoid having to train for  different pulse shapes, depth dependent attenuation, and other pulse parameters that may vary across patients and even across probes as they age. I will discuss the rationale in detail in Chapter 2.

1.5 Organization

Chapter 2 discusses background on deep neural networks and related work on noise suppression with deep learning and CNN-based beamforming. Chapter 3 describes the training data generation process and signal grouping. Chapter 4 explains the CNN architectures and the training pipeline, including a random hyperparameter search technique. Chapter 5 details the beamforming pipeline for evaluation. Chapter 6 addresses the limitations of this work, discusses the results, and concludes the thesis with potential future work.

Chapter 2

Background

2.1 Classic Acoustic Clutter Suppression Algorithms

2.1.1 Tissue Harmonic Imaging

One widely-used approach to suppress cluttered reverberation signals is tissue harmonic imaging (THI). THI circumvents the inherent reverberation in the commonly used fundamental frequency (f_c) by adopting a higher frequency - the second harmonic frequency (f_{hc}). Because reverberation clutter primarily occurs at the fundamental frequency, reflected signals received at a second harmonic frequency are not subject to the same clutter [7, 8, 9]. As a result, harmonic B-mode images have better quality with higher contrast, improved resolution, and less near-field artifact. However, the tradeoffs of higher frequency are higher

attenuation¹ and lower amplitude which cause a loss in axial resolution [10, 11, 12, 13, 14].

In addition, the narrowed bandwidth (fewer frequencies) reduces axial resolution² [15].

2.1.2 Time-Reversal Technique

Time-reversal is another method for suppressing reverberation clutter. In this method, ultrasound waves are transmitted and received twice. After the initial transmit and receive, the signals are reversed and re-transmitted into the field of view. The re-transmitted signals propagate back and refocus on the original source throughout the same medium, subject to the same reverberation. While clutter noises present differently for each transmit (incoherent), non-clutter signals follow the similar frequency patterns (coherent). This approach sums the original and the re-transmitted signals, amplifying signal and reduces reverberation clutter thanks to the constructive and destructive interference of waves depending on coherence. The limitation for this approach is its requirement for a point-like source in the medium as the focal region is difficult to determine [16, 17].

2.1.3 Second-Order Ultrasound Field

Second-order ultrasound field (SURF) is another method for suppressing reverberation clutter in images [18]. This application is specific to contrast-enhanced ultrasound (CEUS),

¹Attenuation is the loss of power (amplitude) as a wave travels through depth. In soft tissue, higher frequency exacerbates attenuation.

²Axial resolution is the measure of how close two scatters are along the depth dimension. Axial resolution is a function of pulse length as well as transducer frequency.

where patients ingest contrast agents to typically in the form of microbubbles and by injection. The goal of CEUS is the detection of the contrast agent instead of tissues. SURF first transmits a low-frequency pulse that alters the scattering properties of the microbubbles. It then use a high-frequency pulse to detect the difference in scattering caused by the low-frequency pulse. This method effectively measures the true depth of the microbubbles while avoiding reverberation clutter in resulting images [19]. The downside of using a high-frequency pulse for imaging is the existence of grating lobes ³, which in turn cause off-axis artifacts. Furthermore, SURF imaging only applies to CEUS and requires a specialized transducer array to emit dual-band waves [16].

2.1.4 Short-Lag Spatial Coherence

Short-lag spatial coherence (SLSC) is a beamforming technique that takes advantage of the spatial similarity among the response waves across the aperture [1]. Instead of summing across the channels as is the case in delay-and-sum (DAS) beamforming, SLSC measures - for each beam - the average correlation between all pairs of channels separated by l ("lag") elements, for a given set of lags. The rationale behind this approach is that adjacent channel signals (short lags) are coherent spatially ⁴, but noises are incoherent. Weighted multiplication of waves would amplify the coherent components (the desired signals) and suppress the incoherent ones (the noises). As a result, the beaformed images show higher contrast,

³Strong side lobes.

⁴Coherent means similar. Coherent waves have the same shape but are separated by a time delay. Coherence is a form of correlation or covariance between waves.

improved contrast-to-noise ratios, and better image texture [20]. The tradeoffs for these improvements include more computational complexity from additional matrix-based correlation derivation and loss in image resolution from only utilizing partial aperture information [21]. Moreover, the values in the image matrix are correlation measures instead of dB. Therefore, SLSC images are not directly comparable to B-mode images.

2.1.5 Coherence Factor

Coherence factor (CF) is a post-processing technique that computes a weight for each beam and each depth and applies these weights to the delay-and-sum (DAS) beamformed RF data [22, 23]. Mathematically, the CF is the ratio of the sum of coherent signals over all signals in each beam. Similar to SLSC, CF takes advantage of the high-coherence property of non-clutter signals to suppress cluttered signals. Compared with SLSC, this method improves image contrast while avoiding introducing of high computational complexity [16].

2.1.6 Minimum-Variance Beamforming

Minimum variance (MV) beamforming is an approach to suppress off-axis scattering. It does so by minimizing the power (the zero-mean variance) of off-axis regions, while preserving the power of the target region (a point location) [24, 25]. MV has proven effective in improving contrast in phantom targets. The drawback of MV is its sensitivity to the dB variation from inside the focal region. In addition, the image quality improvements do not translate to *in*

vivo images.

2.2 Machine Learning-Based Acoustic Clutter Suppression Algorithms

2.2.1 ADMIRE

Aperture Domain Model Image Reconstruction (ADMIRE) is a model-based approach to suppress both off-axis scattering and reverberation clutter. It operates on frequency-domain channel data, decomposes the cluttered signal, selects the scatterer in the region of interest (ROI), and reconstructs the decluttered signal. It then uses regression to determine the coefficient for regularizing each component signal. ADMIRE proves highly effective in suppressing both off-axis scattering and reverberation clutter. However, the computational complexity inherent in this approach precludes real-time applications until further optimization can increase the frame rate [16, 2].

2.2.2 Regularized Inverse

Another machine learning-based approach is regularized inverse, or least squares (LS) beamforming. Given the steering angles⁵ *a priori*, this approach modeled each scanline⁶ in the

⁵Steering angles are the directions of transducer elements in a beam such that the elements form a curved wavefront for focused imaging. They are closely related to time delays.

⁶A scanline in a beam, at a particular depth, consists of signals across the aperture.

DAS beamformed RF data as a function of the scatterer’s peak signal (desired), the given steering matrix, and a Gaussian error term. Stacking the per-depth least squares solutions to the model, the LS approach produces images with improved contrast-to-noise ratios (CNR) [26].

2.3 Deep Learning-Based Acoustic Clutter

Suppression Algorithm

2.3.1 Introduction to Neural Networks

Neural networks are machine learning models that learn by backpropagating loss. They are theoretically able to learn a broad set of complex functions by using nonlinear activations [27]. Convolutional Neural Networks (CNNs) are special neural networks that take advantage of localized parameter sharing, requiring fewer parameters and thus having a reduced risk of overfitting. CNNs have seen widespread applications in Computer Vision, Natural Language Processing, and Medical Imaging alike.

LeNet is the first influential CNN architecture for classifying images. It consists of two convolutional layers followed by two fully-connected ones. Each convolutional layer is followed by a pooling layer for down-sampling. This small architecture was successfully used to recognize handwritten digits [28]. Another early architecture is AlexNet with 5 convolutional layers followed by fully-connected ones [krizhevsky2012imagenet], which

became the first neural-network winner for the ImageNet Large-Scale Visual Recognition Challenge (ILSVRC) in 2012.

2.3.2 Random Hyperparameter Search

Training neural networks involves selecting training and model hyperparameters such as learning rate, dropout rate, and the width of fully-connected layers. Recent studies show that random search is more effective than grid search in finding the optimal neural network [29]. Furthermore, as there are no established models for ultrasound beamforming, a random search for hyperparameters in model architecture, such as the kernel dimensions, the number of kernels, and the padding/stride dimensions for a convolutional layer may be necessary.

2.3.3 CNN Architectures

Most well-known CNN architectures have fully-connected layers after convolutional ones. However, it is not always clear that full connections are necessary as they flatten the spatial features detected by the convolutional layers. There are two notable architectures that avoids using fully-connected layers: the Fully Convolutional Network (FCN) [long2015fcn] and U-Net [ronneberger2015unet]. Both were proposed to solve the problem of semantic segmentation or pixel-wise image classification, while U-Net focuses on biomedical images. Although they differ in architecture, both feature bottlenecks/encoder-decoders and upsampling layers in order to bring the shrunk convolutional outputs back to the size of the input.

The bottleneck layer is an intermediate layer that reduces the size of data coming from its previous layer. Bottleneck layers are used to obtain a (nonlinear) representation of the input with reduced dimensionality, i.e., performing dimension reduction. An example bottleneck layer is an autoencoder, which is used to reduce the previous output and is in turn used to generate a larger encoding that approximates the original input (hence "auto") [ballard1987modular]. For example, the GoogLeNet architecture that won the ImageNet Large-Scale Visual Recognition Challenge 2014 (ILSVRC2014) features 1 by 1 convolutional blocks (termed "network-in-networks" or NiNs) that reduce the number of features before the computationally expensive parallel blocks. [szegedy2015going]. This bottleneck-upsampling approach is a promising network design element that could also be applied to regression tasks because it enables output sizes to match the input.

2.3.4 Convolutional Neural Networks for General Regression

One example CNN solution to a regression task is image orientation prediction. Fischer et al. proposed an approach to train a modified AlexNet to output the sine y and cosine x of an input image. However, in their experiments they found that a single CNN performed poorly compared with a hybrid classification-regression method that performed better than non-neural network approaches, albeit with a nontrivial error rate [fischer2015image].

2.3.5 Multi-Layer Perceptrons for Suppressing Off-Axis

Scattering

Recently, Luchies and Byram proposed a neural-network approach to suppress off-axis scattering [3, 30]. They trained multi-layer perceptrons (MLPs) that operated in the short-time Fourier transform (STFT)⁷ domain to suppress the off-axis signals based on simulated point targets. These beamformers are convolutional in nature insofar as the networks, including their weights, are reused through depth; however, fully-connected layers are used to span the aperture dimension. This method proved effective in improving contrast while preserving speckle patterns. This work motivates further exploration of CNNs on the same STFT-domain data, as there may be spatial features in the frequency domain that could be more effectively learned by CNNs, such as aperture shapes. In addition, training in the STFT domain helps avoid having to train for experimental parameters such as different pulse shapes and depth dependent attenuation.

2.3.6 Convolutional Neural Networks for Beamforming

There are two notable related CNN-based approaches for reducing off-axis scattering, learning ultrasound reconstruction, and speckle reduction. For example, Yoon et al. proposed a method that effectively interpolates missing sub-sampled RF data in 3D ultrasound [31].

Hyun et al. showed that fully-convolutional neural networks (FCNs) have the potential to

⁷Frequency.

learn a speckle-reducing beamformer which also suppresses off-axis scattering. Their learning task is to beamform a B-mode image from raw RF data. Their networks used between 2 and 16 convolutional layers with same padding in order to preserve the input dimensionality throughout the network. Notably, they explored different loss functions including L1, L2, SSIM, and MS-SSIM losses. They were able to show SNR improvements in both phantom and *in vivo* targets. However, the images did not indicate clear CNR improvements for all targets [32].

Bibliography

- [1] Muyinatu A Lediju et al. “Short-lag spatial coherence of backscattered echoes: Imaging characteristics”. In: *IEEE transactions on ultrasonics, ferroelectrics, and frequency control* 58.7 (2011), pp. 1377–1388.
- [2] Brett Byram et al. “A model and regularization scheme for ultrasonic beamforming clutter reduction”. In: *IEEE transactions on ultrasonics, ferroelectrics, and frequency control* 62.11 (2015), pp. 1913–1927.
- [3] A. C. Luchies and B. C. Byram. “Deep Neural Networks for Ultrasound Beamforming”. In: *IEEE Transactions on Medical Imaging* 37.9 (Sept. 2018), pp. 2010–2021. DOI: 10.1109/TMI.2018.2809641.
- [4] Olaf Ronneberger, Philipp Fischer, and Thomas Brox. “U-net: Convolutional networks for biomedical image segmentation”. In: *International Conference on Medical image computing and computer-assisted intervention*. Springer. 2015, pp. 234–241.
- [5] R. J. G. van Sloun, R. Cohen, and Y. C. Eldar. “Deep Learning in Ultrasound Imaging”. In: *Proceedings of the IEEE* (2019), pp. 1–19. DOI: 10.1109/JPROC.2019.2932116.

- [6] D. Hyun et al. “Beamforming and Speckle Reduction Using Neural Networks”. In: *IEEE Transactions on Ultrasonics, Ferroelectrics, and Frequency Control* 66.5 (May 2019), pp. 898–910. DOI: 10.1109/TUFFC.2019.2903795.
- [7] Ted Christopher. “Finite amplitude distortion-based inhomogeneous pulse echo ultrasonic imaging”. In: *IEEE transactions on ultrasonics, ferroelectrics, and frequency control* 44.1 (1997), pp. 125–139.
- [8] B. Ward, A. C. Baker, and V. F. Humphrey. “Nonlinear propagation applied to the improvement of resolution in diagnostic medical ultrasound”. In: *The Journal of the Acoustical Society of America* 101.1 (1997), pp. 143–154. DOI: 10.1121/1.417977. eprint: <https://doi.org/10.1121/1.417977>. URL: <https://doi.org/10.1121/1.417977>.
- [9] M. A. Averkiou, D. N. Roundhill, and J. E. Powers. “A new imaging technique based on the nonlinear properties of tissues”. In: *1997 IEEE Ultrasonics Symposium Proceedings. An International Symposium (Cat. No.97CH36118)*. Vol. 2. Oct. 1997, 1561–1566 vol.2. DOI: 10.1109/ULTSYM.1997.663294.
- [10] TG Muir and EL Carstensen. “Prediction of nonlinear acoustic effects at biomedical frequencies and intensities”. In: *Ultrasound in medicine & biology* 6.4 (1980), pp. 345–357.

- [11] HC Starritt et al. “The development of harmonic distortion in pulsed finite-amplitude ultrasound passing through liver”. In: *Physics in Medicine & Biology* 31.12 (1986), p. 1401.
- [12] Victor F Humphrey. “Nonlinear propagation in ultrasonic fields: measurements, modelling and harmonic imaging”. In: *Ultrasonics* 38.1-8 (2000), pp. 267–272.
- [13] Richard SC Cobbold. *Foundations of biomedical ultrasound*. Oxford university press, 2006.
- [14] Arash Anvari, Flemming Forsberg, and Anthony E Samir. “A primer on the physical principles of tissue harmonic imaging”. In: *Radiographics* 35.7 (2015), pp. 1955–1964.
- [15] TA Whittingham. “Tissue harmonic imaging”. In: *European radiology* 9.3 (1999), S323–S326.
- [16] Kazuyuki Dei. “Model-Based Ultrasound Imaging for Challenging Acoustic Clutter Suppression”. PhD thesis. Vanderbilt University, 2019.
- [17] Mathias Fink. “Time reversal of ultrasonic fields. I. Basic principles”. In: *IEEE transactions on ultrasonics, ferroelectrics, and frequency control* 39.5 (1992), pp. 555–566.
- [18] Bjørn AJ Angelsen and Rune Hansen. “7A-1 SURF Imaging-A new method for ultrasound contrast agent imaging”. In: *2007 IEEE Ultrasonics Symposium Proceedings*. IEEE. 2007, pp. 531–541.

- [19] S. Masoy et al. “SURF imaging: In vivo demonstration of an ultrasound contrast agent detection technique”. In: *IEEE Transactions on Ultrasonics, Ferroelectrics, and Frequency Control* 55.5 (May 2008), pp. 1112–1121. DOI: 10.1109/TUFFC.2008.763.
- [20] Jeremy J Dahl et al. “Coherence beamforming and its applications to the difficult-to-image patient”. In: *2017 IEEE International Ultrasonics Symposium (IUS)*. IEEE. 2017, pp. 1–10.
- [21] M. A. Lediju Bell, J. J. Dahl, and G. E. Trahey. “Resolution and brightness characteristics of short-lag spatial coherence (SLSC) images”. In: *IEEE Transactions on Ultrasonics, Ferroelectrics, and Frequency Control* 62.7 (July 2015), pp. 1265–1276. DOI: 10.1109/TUFFC.2014.006909.
- [22] Raoul Mallart and Mathias Fink. “Adaptive focusing in scattering media through sound-speed inhomogeneities: The van Cittert Zernike approach and focusing criterion”. In: *The Journal of the Acoustical Society of America* 96.6 (1994), pp. 3721–3732.
- [23] KW Hollman, KW Rigby, and M O’donnell. “Coherence factor of speckle from a multi-row probe”. In: *1999 IEEE Ultrasonics Symposium. Proceedings. International Symposium (Cat. No. 99CH37027)*. Vol. 2. IEEE. 1999, pp. 1257–1260.
- [24] Johan Fredrik Synnevag, Andreas Austeng, and Sverre Holm. “Adaptive beamforming applied to medical ultrasound imaging”. In: *IEEE transactions on ultrasonics, ferroelectrics, and frequency control* 54.8 (2007), pp. 1606–1613.

- [25] Iben Kraglund Holfort, Fredrik Gran, and Jorgen Arendt Jensen. “Broadband minimum variance beamforming for ultrasound imaging”. In: *IEEE transactions on ultrasonics, ferroelectrics, and frequency control* 56.2 (2009), pp. 314–325.
- [26] T. Szasz, A. Basarab, and D. Kouamé. “Beamforming Through Regularized Inverse Problems in Ultrasound Medical Imaging”. In: *IEEE Transactions on Ultrasonics, Ferroelectrics, and Frequency Control* 63.12 (Dec. 2016), pp. 2031–2044. DOI: 10.1109/TUFFC.2016.2608939.
- [27] David E Rumelhart, Geoffrey E Hinton, and Ronald J Williams. *Learning internal representations by error propagation*. Tech. rep. California Univ San Diego La Jolla Inst for Cognitive Science, 1985.
- [28] Yann LeCun et al. “Gradient-based learning applied to document recognition”. In: *Proceedings of the IEEE* 86.11 (1998), pp. 2278–2324.
- [29] James Bergstra and Yoshua Bengio. “Random search for hyper-parameter optimization”. In: *Journal of Machine Learning Research* 13.Feb (2012), pp. 281–305.
- [30] Adam C Luchies and Brett C Byram. “Training improvements for ultrasound beamforming with deep neural networks”. In: *Physics in medicine and biology* (2019).
- [31] Yeo Hun Yoon et al. “Efficient b-mode ultrasound image reconstruction from subsampled rf data using deep learning”. In: *IEEE transactions on medical imaging* 38.2 (2018), pp. 325–336.

- [32] Dongwoon Hyun et al. “Beamforming and Speckle Reduction Using Neural Networks”.
In: *IEEE transactions on ultrasonics, ferroelectrics, and frequency control* 66.5 (2019),
pp. 898–910.